

pH-Responsive Shrinkage/Swelling of a Supramolecular Hydrogel Composed of Two Small Amphiphilic Molecules

Shan-Lai Zhou,^[b] Shinji Matsumoto,^[b] Huai-Dong Tian,^[b] Hiroki Yamane,^[b] Akio Ojida,^[b] Shigeki Kiyonaka,^[b] and Itaru Hamachi^{*,[a]}

Abstract: A pH-responsive volume-change function was successfully introduced into a supramolecular hydrogel that contained GalNAc-appended (GalNAc = *N*-acetylgalactosamine) glutamate ester **1** by the simple mixing of it with an appropriate amount of **2a** or **2b** amphiphilic carboxylic acid. In the 1:1 mixture (**1:2**), the hydrogel swelled under neutral pH conditions, but shrank to almost half of its original volume under acidic pH conditions. The structure and pH response of the mixed hydrogel were characterized by

using X-ray diffraction (XRD), confocal laser scanning microscopy (CLSM), transmission or scanning electron microscopy (TEM, SEM), and Fourier transform IR (FTIR) spectroscopy. Well-developed fibers formed a stable hydrogel by self-assembly, and under acidic conditions the charge of the carboxylic acid terminal (from the carbox-

ylate anion) was neutralized and then these fibers became densely packed. This macroscopic pH response was also applied to the pH-triggered release of bioactive substances. In this mixed supramolecular hydrogel, the hydrogelator **1** provides a stable hydrogel structure and the additive **2** acts as a commander that is sensitive to an environmental pH signal. The present supramolecular copolymerization strategy should be useful for the construction of novel, stimuli-responsive, soft materials.

Keywords: carboxylic acids • copolymerization • gels • pH response • supramolecular chemistry

Introduction

The development of stimuli-responsive, synthetic molecules for the construction of molecular memories, switches, and machines^[1–3] has been ongoing for more than two decades. Nevertheless, substantial discrepancies between sophisticated molecules in solution and macroscopic materials displaying a macroscopic response have been recognized and investigated. In a pioneering approach, Stoddart and co-workers created a monolayer assembly consisting of catenanes or ro-

taxanes, which could operate as a switch device to regulate macroscopic electric capacity.^[4] Further efforts are, however, required before these small molecules can be applied to molecularly defined, macroscopic devices. Most stimuli-responsive, macroscopic materials are synthesized from polymers,^[5] even though precise manufacturing is generally difficult in polymer-based materials. Supramolecular polymers (noncovalently assembled, polymeric molecules) are regarded as intermediates between molecules and conventional polymers; therefore, it is envisioned that molecularly defined, intelligent materials may be constructed by using the supramolecular concept.^[6]

We recently discovered a supramolecular polymer in the form of a new hydrogel consisting of a low-molecular-weight, glycosylated amino acetate (a so-called supramolecular hydrogel) that displayed a unique property of thermally induced, volume phase transition.^[7] Stimuli-responsive, macroscopic shrinkage/swelling in polymer-based hydrogels was pioneered by T. Tanaka, and the potential use of such gels as soft materials in diverse applications has been anticipated.^[8] In contrast, few studies of responsive volume change have been performed in supramolecular hydro- or organogels, although there are many reports of responsive gel-sol transitions.^[9,10] This may be because noncovalent interac-

- [a] Prof. I. Hamachi
PRESTO (Synthesis and Control, JST)
Institute for Materials Chemistry and Engineering (IMCE)
Department of Chemistry and Biochemistry
Graduate School of Engineering
Kyushu University, Fukuoka 812-8581 (Japan)
Fax: (+81) 92-642-2715
E-mail: itarutcm@mbox.nc.kyushu-u.ac.jp
- [b] S.-L. Zhou, S. Matsumoto, Dr. H.-D. Tian, H. Yamane, Dr. A. Ojida, Dr. S. Kiyonaka
Department of Chemistry and Biochemistry
Graduate School of Engineering, Kyushu University
Fukuoka 812-8581 (Japan)

Supporting information for this article is available on the WWW under <http://www.chemeurj.org/> or from the author.

tions, relative to covalent ones, are generally too weak to maintain stable polymeric chains prior to and following stimuli, and instead readily degrade into nonpolymeric units producing a sol state but no volume change. Our report of the thermal shrinkage of a supramolecular hydrogel suggested, however, that a thermally stable, noncovalent polymer chain composed of multiply accumulated interactions can display thermal shrinkage instead of simply dissolving.^[7a,11] The design at the molecular level of such a unique feature will provide a new category of supramolecular materials. From this perspective, we have investigated supramolecular systems that exhibit various stimuli-responsive volume changes. We recently reported the addition of a carboxylic acid derivative to the supramolecular gelator matrix to form a highly stable, self-assembled nanofiber in small amounts. This matrix revealed pH-dependent, thermal behavior of the mixed hydrogel, that is, gel–sol transition at neutral pH and volume phase transition at acidic pH.^[9a] Here we describe the successful pH-triggered shrinkage or swelling of a supramolecular hydrogel, which was produced by mixing optimized structures and amounts of amphiphilic carboxylic acids with the hydrogelator. This supramolecular copolymerization strategy is widely applicable for the production of novel, stimuli-responsive, supramolecular materials.^[12]

Results and Discussion

Molecular design and gelation screening: GalNAc-appended (GalNAc = *N*-acetylgalactosamine) glutamate ester **1** (which was found by using a combinatorial approach to be an excellent, low-molecular-weight hydrogelator) was used as the fundamental gel matrix, because of its stable, nanofiber formation.^[11,13] As an additional component, three amphiphilic carboxylic acid derivatives bearing different lengths of methylene chains (**2a–c**) were designed and synthesized on the basis of their structural similarity to the hydrophobic parts of **1**. Figure 1a shows the gelation capabilities of the mixed gels under neutral pH conditions. A single component of **2a–c** (i.e., molar ratio **1/2** = 0:10) is quite soluble in water and, therefore, has no gelation capability with water. On the other hand, a single component of **1** (i.e., molar

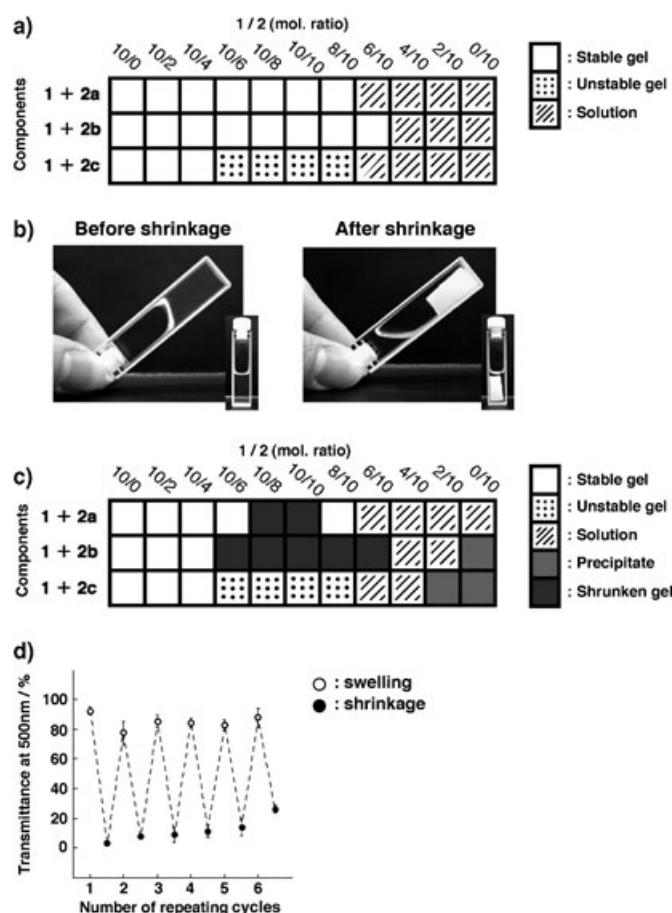
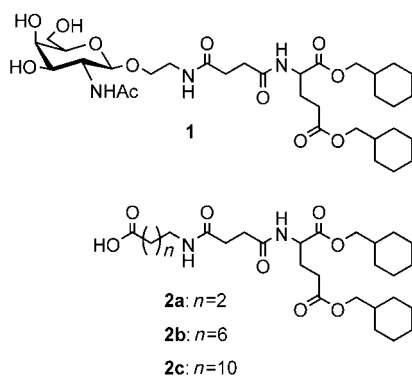


Figure 1. a) Gelation screening of the mixed hydrogels consisting of **1** and **2a**, **b**, or **c**. The content of the total components (**1** + **2**) is 0.5 wt % in all cases. The stable hydrogel was not displaced upon inversion of the test tube, whereas the unstable hydrogel collapsed. b) Photographs of a typical example of the pH-responsive volume phase transition of the mixed hydrogel (**1/2b** = 10:10) before and after shrinkage. c) Screening of the pH-responsive volume-change function of the mixed hydrogel performed as in a). d) Repeated shrinkage/swelling cycles resulting from a change in pH and monitored by measuring gel transparency. The average values and experimental errors from three independent experiments were plotted.

ratio **1/2** = 10:0) forms a stable hydrogel. The mixing of these components in various ratios produces solutions with distinct macroscopic phases, such as a homogeneous solution, an unstable hydrogel, and a stable hydrogel, depending on the ratio of mixing. Stable gels were formed following the mixing of a single component of **1** and an almost equimolar amount of **2**. The gelation capability of the mixed hydrogel is also influenced by the molecular structure of **2**. The mixture of **2b** and **1** gels neutral water over the widest ratio range among the three derivatives (**1/2b** = 10:0–6:10). The addition of excess **2** (**1/2a** > 8:10, **1/2b** > 6:10, **1/2c** > 8:10) produces a homogeneous solution instead of a hydrogel. In the case of **2c**, which has the longest methylene chain, the almost equimolar mixture ratios (**1/2c** = 10:6–8:10) produced unstable hydrogels.

pH-Induced shrinkage of the two-component hydrogel: The hydrogels were exposed to an acidic atmosphere (HCl vapor) and changes in their macroscopic morphology were observed. A typical example is shown in Figure 1b. Clearly, shrinkage of the hydrogel takes place upon exposure to an acidic vapor. Half of the volume of water was expelled from the original hydrogel. In addition, the hydrogel changes from almost transparent to opaque, and the shrunken gel becomes stiffer than the original, swollen gel. As shown in Figure 1c, such gel-shrinkage occurs only in those mixed hydrogels with almost equimolar ratios of **1** and **2**, and was not observed in the single component of **1** or in mixtures containing the small amounts of **2**. This implies that the pH response requires both components to be present in an optimal ratio. Interestingly, the pH-responsive volume change was also sensitive to the molecular structure of the additive **2**. The addition of **2b** affords pH-responsive gel shrinkage over the widest ratio range among the three additives (10:6–6:10), whereas **2a**, which bears the shortest methylene unit, causes a macroscopic pH response of the hydrogel within a rather limited range (10:8–10:10), and **2c**, with the longest methylene chain, confers no pH-sensitive gel shrinkage at all. This trend is in good agreement with the data obtained for the gelation capability (Figure 1a). By using molecular modeling to compare the molecular lengths of **1** and **2**, it is suggested that the hydrophilic carboxylic acid group in the case of **2b** is slightly exposed at its interface with the hydrophilic GalNAc groups of **1**, but slightly buried in the case of **2a**, and very exposed in the case of **2c**.^[14] It is interesting that such a subtle structural difference appears to significantly influence not only the gelation capability, but also the resultant pH response of the mixed hydrogel. Another control sample, in which the methyl ester of **2b** was mixed with **1** in an equimolar ratio, displayed no pH-responsive volume change. We also tested the formation of a **1/2b** (1:1 ratio) hydrogel under acidic pH conditions (pH 4.0), which resulted in a shrunken, opaque gel comparable to the pH-triggered shrunken gel. These results suggest that the charge alteration (from negative to neutral) at the interface is crucial for the pH-responsive volume change.

The shrunken hydrogel was re-swelled and became almost transparent by neutralization with neutral buffer solution (pH 7), followed by slight warming (40 °C). The shrinkage/swelling cycle can be repeated at least six times (Figure 1d), as monitored by the change in transparency. The ability to repeat the cycle indicates that the pH-induced gel shrinkage is not caused by the chemical decomposition of the component,^[15] but by a reversible, physicochemical property change in the mixed hydrogel.

Structural analysis of the two-component hydrogel: The structure of the mixed supramolecular hydrogel was examined by using several microscopy and spectroscopy techniques. The X-ray diffraction pattern (XRD, Figure 2) of the mixed hydrogel displayed two peaks corresponding to 3.7 nm (2.4°) and 0.4 nm (19.8°), values that are almost comparable to those obtained for the single-component hydrogel

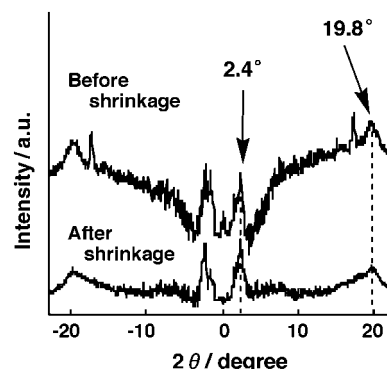


Figure 2. XRD profiles of the mixed hydrogel (**1/2b**=10:10) before and after gel shrinkage.

of **1**.^[16] From our previous study of **1**, based on XRD data and single crystal analysis, these values can be reasonably assigned to the interdigitated bimolecular layer of **1** (3.7 nm) and the van der Waals packing distance of the cyclohexyl rings of the hydrophobic core (0.4 nm).^[11] Interestingly, good agreement between the long spacing in the mixed hydrogel with that of the single-component hydrogel **1** indicates that the two-component hydrogel of **1** and **2b** has a fundamental, bilayer-like structure comparable to the single-component hydrogel **1**.^[17] Significantly, similar XRD peaks appear in the spectra for the shrunken gel, suggesting that the fundamental packing mode is not significantly disturbed by the pH-induced volume change.

Confocal laser scanning microscopy (CLSM) produces a wet gel morphology without a drying process. Figure 3a shows a typical image of the mixed hydrogel that has been stained by a nitrobenzoxadiazole derivative (HANBD), an environmentally sensitive fluorophore that emits a strong fluorescence with a blue-shifted wavelength in less polar environments. Long fibers with green fluorescence were observed. The fluorescence spectrum of the area proximal to a fiber (circled in Figure 3a), shows the stronger peak at 530 nm with a shoulder at 550 nm (Figure 3b). Compared to the maximum peak of HANBD in aqueous solution (550 nm), the presence of the mixed hydrogel causes a blue-shift of 20 nm, which strongly suggests that HANBD is incorporated into a hydrophobic domain of the hydrogel fibers, resulting in a strong emission. The shoulder peak at 550 nm implies that HANBD molecules partially distribute in the aqueous region of the hydrogel. The continuous hydrophobic region is consistent with the mixed hydrogel structure suggested by the XRD data described above. A greater blue-shift in the single-component hydrogel **1** is observed at 525 nm, indicating that the well-developed hydrophobic domains are slightly disturbed by **2b** in the mixed hydrogel.

Thin fibers (10–100 nm diameter) of the mixed hydrogel (**1/2b**=10:10), under both neutral and acidic conditions, were also observed by using transmission electron microscopy (TEM, Figure 4a and b, respectively). This fibrous morphology is almost the same as that of the single-component

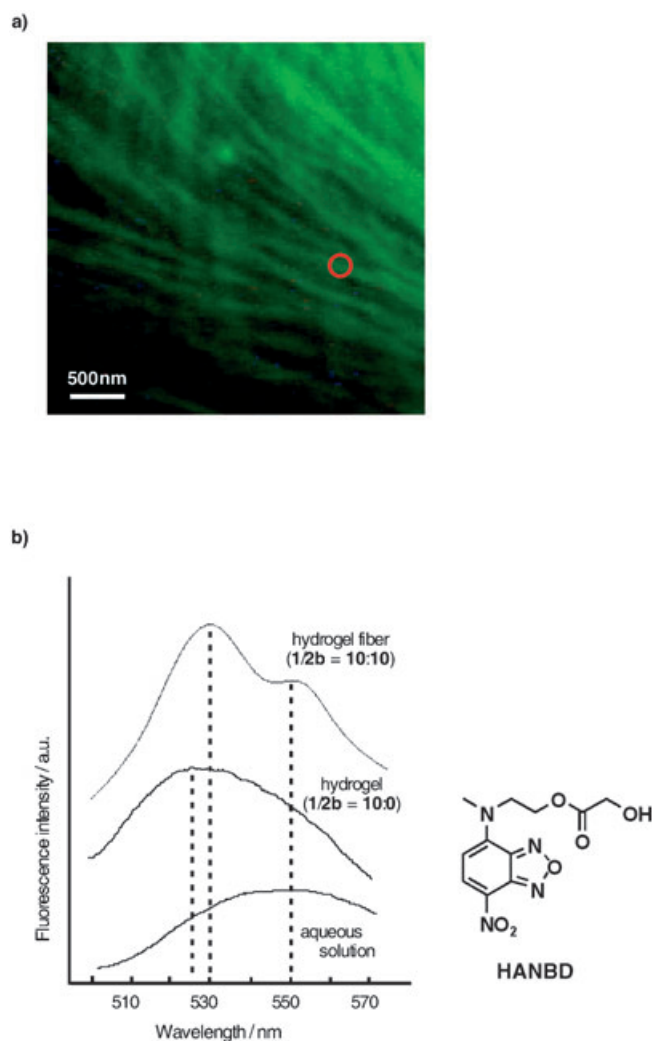


Figure 3. a) CLSM image of the hydrogel ($1/2b=10:10$, 0.5 wt %) containing 20 μM HANBD under neutral pH conditions (in pH 7.0 phosphate buffer). The white bar represents a distance of 500 nm. b) Fluorescence spectra of the hydrogel fibers circled in a) ($1/2b=10:10$, 0.5 wt %, measured by using CLSM), the single-component hydrogel **1** ($1/2b=10:0$, 0.5 wt %) containing HANBD, and HANBD in aqueous solution (measured by using the conventional fluorescence spectrophotometer).

hydrogel **1**, indicating that the original self-assembly characteristics are not disrupted by the additive **2b**. Interestingly, the fibers in acidic pH become more densely entangled than those in neutral pH. Entangled, fibrous, three-dimensional networks were observed by using scanning electron microscopy (SEM, Figure 4c and d). Consistent with TEM observations, fibers in acidic pH conditions become thicker than those in neutral conditions. These results suggest that the macroscopic opaqueness of the hydrogel may be ascribed to a thickening of the pH-induced fibrils, caused by the dense packing of the self-assembled fibers.

FTIR measurements of the mixed hydrogel before and after shrinkage show a significant change in the equilibrium between the carboxylic acid (COOH) and the carboxylate ion (COO^-) (Figure 5). In the shrunken gel, a shoulder peak

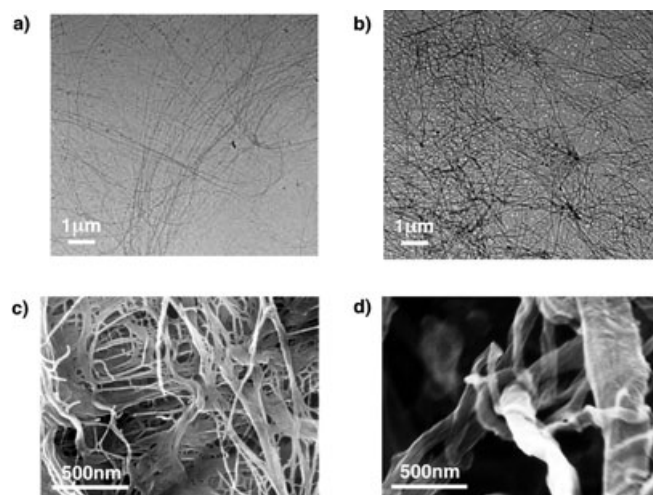


Figure 4. TEM images of the unstained a) swollen and b) shrunken hydrogel ($1/2b=10:10$, 0.5 wt %). A piece of the gel was placed on a carbon-coated, copper grid and dried for 6 h. SEM images of the c) swollen and d) shrunken hydrogel ($1/2b=10:10$, 0.5 wt %), which had been coated by platinum vapor deposition (30 s). For SEM samples, the swollen and shrunken hydrogel was frozen in liquid nitrogen and then lyophilized in vacuo for 1 day.

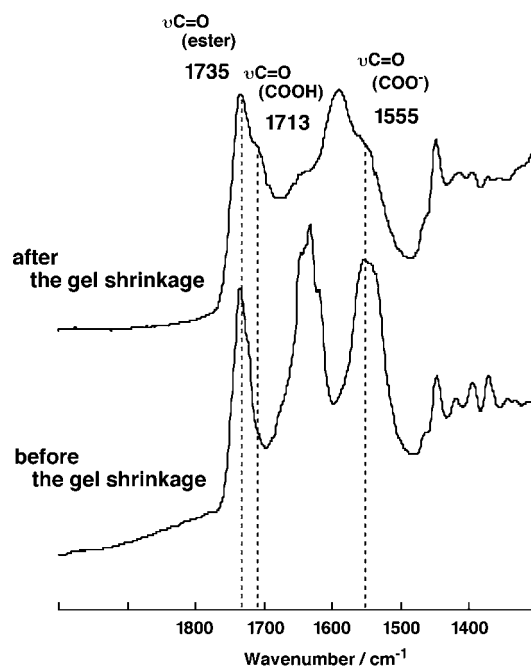


Figure 5. FTIR spectra of the mixed hydrogel ($1/2b=10:10$, 0.5 wt %) before and after gel shrinkage.

at 1713 cm^{-1} appears, which originates from the stretching of the dimeric COOH, whereas a strong peak at 1555 cm^{-1} , due to COO^- , disappears.^[18] This result indicates that the charged carboxylate state of **2b** shifts to the neutral carboxylic acid state by exposure of the hydrogel to the acidic atmosphere. It may be reasonable to propose that, in addition to increased osmotic pressure caused by the incorporation

of a counter cation, the charged gel fiber causes an interfibrous repulsion to yield a swollen gel. In contrast, suppression of such electrostatic repulsion and the decrease in osmotic pressure caused by the release of counterions in the neutral fiber, results in hydrogel shrinkage upon charge neutralization.^[8a,d] This explanation is supported by the observation that the inclusion of the methyl ester of **2b** induced no pH response in the mixed hydrogel.

pH-Responsive drug release of the supramolecular hydrogel: Next, we investigated the pH-triggered release of bioactive substances.^[19] Water-soluble vitamins, such as vitamins B₁, B₆, and B₁₂, were entrapped in the mixed hydrogel (**1/2b**=10:10) as hydrophilic guest molecules during the gel preparation process, and the environmental pH was gradually acidified. The time course of vitamin B₁₂ release upon acidification was quantitatively determined by using UV-visible spectroscopy (Figure 6a). Under neutral conditions,

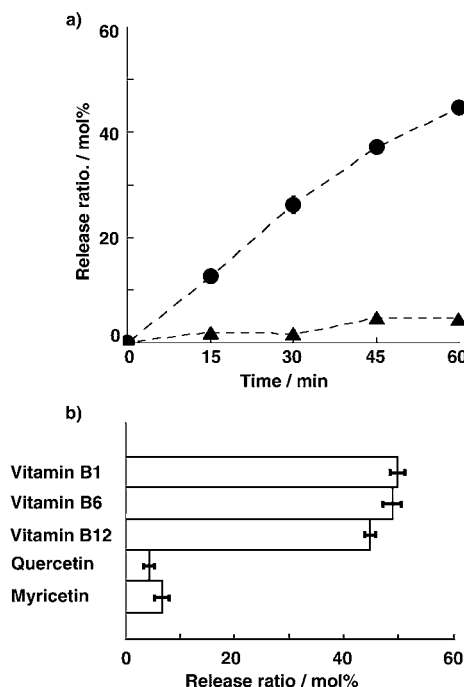


Figure 6. a) Time courses of the release of vitamin B₁₂ (●) and quercetin (▲) substrates from the mixed hydrogel (**1/2b**=10:10), caused by pH-triggered gel shrinkage. b) The amount of five distinct substrates released after 60 min for vitamin B₁ (thiamine pyrophosphate), vitamin B₆ (pyridoxal 5'-phosphate), vitamin B₁₂ (cyanocobalamin), quercetin (3,3',4',5,7-pentahydroxyflavone), and myricetin (3,3',4',5,5',7-hexahydroxyflavone). In both a) and b) the average values and experimental errors from three independent experiments were plotted.

no release was observed due to the absence of gel shrinkage. Vitamin B₁₂ was released concurrent with gel shrinkage in an acidic atmosphere of HCl vapor. The vitamin B₁₂-entrapped hydrogel shrank by up to one half of its initial volume (see Figure 1b), and almost 50% of the vitamin B₁₂ was released within 60 min. The other two vitamin Bs (Figure 6b) exhibited release behavior similar to that of vitamin B₁₂.

These results indicate that, in pH-triggered release, the vitamins are released in the expelled water. In contrast, the rather hydrophobic flavone derivatives, such as myricetin and quercetin, were less efficiently released, in spite of gel shrinkage (Figure 6a and b). This is because hydrophobic substances localize predominantly in the hydrophobic domain of the supramolecular gel fibers, with a lower amount present in the expelled water. Therefore, controlled release can be performed in this system by employing two controlling factors; pH-induced volume change and the amphiphilic structure of the supramolecular hydrogel.

Conclusion

pH-Responsive characteristics were conferred to a supramolecular hydrogel by simple mixing of a hydrogelator with small acidic molecules. Unlike the supramolecular hydrogels reported by others,^[9] which exhibited gel-sol transitions, the hydrogel described here displays pH-responsive shrinkage or swelling. The pH-induced shrinkage does not occur in the case of single-component hydrogels **1** or **2b**, that is, **1** forms a stable hydrogel without pH sensitivity and **2b** does not form a supramolecular hydrogel. Therefore, it is conceivable that the hydrogelator **1** provides a superior hydrogel matrix, and that the additive **2b** acts as a commander that is sensitive to environmental pH signals in this supramolecular hydrogel. The pH-induced volume change produces controlled drug release. Such a supramolecular copolymerization strategy (Figure 7) could be applied to other systems,^[20] with the aim of designing sophisticated materials that are responsive to various stimuli.

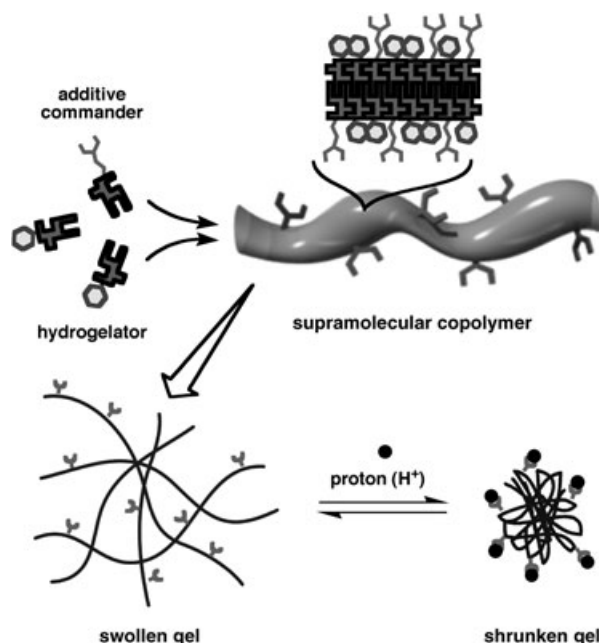


Figure 7. Schematic illustration of the supramolecular copolymerization strategy used to design a hydrogel, and the subsequent pH-responsive volume change.

Experimental Section

Materials and methods: All chemical reagents were obtained from Aldrich, Sigma, TCI, Wako, or Watanabe, and were used without further purification. Solvents were dried according to standard procedure. ^1H NMR spectra were obtained by using a JEOL-JNM-EX400 apparatus (400 MHz). Mass spectra were recorded on a MALDI-TOF mass spectrometer PE Voyager DE-RP. SEM images were obtained by using an Hitachi S-5000, acceleration voltage 25 kV. Conventional fluorescence spectra were recorded by using an Hitachi F-4500 instrument. TEM images were recorded by using a JEOL-JEM-2010 apparatus. FTIR spectra were recorded by using a Perkin-Elmer Spectrum One on ATR mode.

Synthesis: Compounds **1** and **2** were prepared according to the method reported previously.^[9n,13]

Data for 2b: ^1H NMR (400 MHz, CDCl_3 , TMS): δ = 6.81 (d, J = 7.6 Hz, 1H; $\text{COCH}(\text{NH})\text{CH}_2\text{CH}_2\text{CO}$), 6.12 (t, J = 5.2 Hz, 1H; $\text{CHNHCOCH}_2\text{CH}_2\text{CONHCH}_2$), 4.59 (m, 1H; $\text{COCH}(\text{NH})\text{CH}_2\text{CH}_2\text{CO}$), 3.95, 3.89 (d, J = 6.4 Hz, 4H; 6.4 Hz, $\text{COOCH}_2\text{C}_6\text{H}_{11}$), 3.22 (m, 2H; $\text{NHCH}_2(\text{CH}_2)_5\text{CH}_2\text{COOH}$), 2.60–2.32 (m, 8H; $\text{COCH}_2\text{CH}_2\text{CO}$, $\text{COCH}(\text{NH})\text{CH}_2\text{CH}_2\text{CO}$, $\text{NHCH}_2(\text{CH}_2)_5\text{CH}_2\text{COOH}$), 2.22, 1.99 (m, 2H; $\text{COCH}(\text{NH})\text{CH}_2\text{CH}_2\text{CO}$), 1.80–0.91 ppm (m, 32H; $\text{NHCH}_2(\text{CH}_2)_5\text{CH}_2\text{COOH}$, $\text{COOCH}_2\text{C}_6\text{H}_{11}$); MALDI-TOF-MS: m/z : calcd for $\text{C}_{31}\text{H}_{52}\text{N}_2\text{O}_8$: 580.37; found: 603.80 $[\text{M}+\text{Na}]^+$; elemental analysis calcd (%) for $\text{C}_{31}\text{H}_{52}\text{N}_2\text{O}_8$: C64.11, H9.02, N4.82; found: C64.11, H9.02, N4.79.

Data for 2a: ^1H NMR (400 MHz, CDCl_3 , TMS): δ = 6.77 (d, J = 7.2 Hz, 1H; $\text{COCH}(\text{NH})\text{CH}_2\text{CH}_2\text{CO}$), 6.41 (m, 1H; $\text{CHNHCOCH}_2\text{CH}_2\text{CONHCH}_2$), 4.58 (m, 1H; $\text{COCH}(\text{NH})\text{CH}_2\text{CH}_2\text{CO}$), 3.96, 3.89 (d, J = 6.4 Hz, 4H; 6.4 Hz, $\text{COOCH}_2\text{C}_6\text{H}_{11}$), 3.34 (m, 2H; $\text{NHCH}_2\text{CH}_2\text{CH}_2\text{COOH}$), 2.61–2.35 (m, 8H; $\text{COCH}_2\text{CH}_2\text{CO}$, $\text{COCH}(\text{NH})\text{CH}_2\text{CH}_2\text{CO}$, $\text{NHCH}_2\text{CH}_2\text{CH}_2\text{COOH}$), 2.20, 2.00 (m, 2H; $\text{COCH}(\text{NH})\text{CH}_2\text{CH}_2\text{CO}$), 1.89–0.94 ppm (m, 24H; $\text{NHCH}_2\text{CH}_2\text{CH}_2\text{COOH}$, $\text{COOCH}_2\text{C}_6\text{H}_{11}$); FAB-MS: m/z : calcd for $\text{C}_{27}\text{H}_{44}\text{N}_2\text{O}_8$: 524.31; found: 525.40 $[\text{M}+\text{H}]^+$; elemental analysis calcd (%) for $\text{C}_{27}\text{H}_{44}\text{N}_2\text{O}_8$: C61.81, H8.45, N5.34; found: C61.72, H8.43, N5.28.

Data for 2c: ^1H NMR (400 MHz, CDCl_3 , TMS): δ = 6.71 (m, 1H; $\text{COCH}(\text{NH})\text{CH}_2\text{CH}_2\text{CO}$), 6.14 (m, 1H; $\text{CHNHCOCH}_2\text{CH}_2\text{CONHCH}_2$), 4.58 (m, 1H; $\text{COCH}(\text{NH})\text{CH}_2\text{CH}_2\text{CO}$), 3.94, 3.88 (d, J = 6.0 Hz, 4H; 6.4 Hz, $\text{COOCH}_2\text{C}_6\text{H}_{11}$), 3.21 (m, 2H; $\text{NHCH}_2(\text{CH}_2)_9\text{CH}_2\text{COOH}$), 2.60–2.25 (m, 8H; $\text{COCH}_2\text{CH}_2\text{CO}$, $\text{COCH}(\text{NH})\text{CH}_2\text{CH}_2\text{CO}$, $\text{NHCH}_2(\text{CH}_2)_9\text{CH}_2\text{COOH}$), 2.17, 1.97 (m, 2H; $\text{COCH}(\text{NH})\text{CH}_2\text{CH}_2\text{CO}$), 1.80–0.85 ppm (m, 40H; $\text{NHCH}_2(\text{CH}_2)_9\text{CH}_2\text{COOH}$, $\text{COOCH}_2\text{C}_6\text{H}_{11}$); FAB-MS: m/z : calcd for $\text{C}_{35}\text{H}_{60}\text{N}_2\text{O}_8$: 636.43; found: 637.50 $[\text{M}+\text{H}]^+$; elemental analysis calcd (%) for $\text{C}_{35}\text{H}_{60}\text{N}_2\text{O}_8$: C66.01, H9.50, N4.40; found: C65.89, H9.47, N4.37.

Synthesis of methyl ester of 2b: The methyl ester of 8-aminooctanoic acid was used for the condensation step in the synthesis of **2b** to yield the target methyl ester as a colorless solid. ^1H NMR (400 MHz, CDCl_3 , TMS): δ = 6.60 (d, J = 7.6 Hz, 1H; $\text{COCH}(\text{NH})\text{CH}_2\text{CH}_2\text{CO}$), 5.88 (m, 1H; $\text{CHNHCOCH}_2\text{CH}_2\text{CONHCH}_2$), 4.59 (m, 1H; $\text{COCH}(\text{NH})\text{CH}_2\text{CH}_2\text{CO}$), 3.94, 3.88 (d, J = 6.8 Hz, 4H; 6.8 Hz, $\text{COOCH}_2\text{C}_6\text{H}_{11}$), 3.67 (s, 1H; COOCH_3), 3.22 (m, 2H; $\text{NHCH}_2(\text{CH}_2)_5\text{CH}_2\text{COOCH}_3$), 2.58–2.28 (m, 8H; $\text{COCH}_2\text{CH}_2\text{CO}$, $\text{COCH}(\text{NH})\text{CH}_2\text{CH}_2\text{CO}$, $\text{NHCH}_2(\text{CH}_2)_5\text{CH}_2\text{COOCH}_3$), 2.21, 1.99 (m, 2H; $\text{COCH}(\text{NH})\text{CH}_2\text{CH}_2\text{CO}$), 1.80–0.94 ppm (m, 32H; $\text{NHCH}_2(\text{CH}_2)_5\text{CH}_2\text{COOCH}_3$, $\text{COOCH}_2\text{C}_6\text{H}_{11}$); FAB-MS: m/z : calcd for $\text{C}_{32}\text{H}_{54}\text{N}_2\text{O}_8$: 594.39; found: 595.4 $[\text{M}+\text{H}]^+$; elemental analysis of methyl ester calcd (%) for $\text{C}_{32}\text{H}_{54}\text{N}_2\text{O}_8$: C64.62, H9.15, N4.71; found: C64.66, H9.08, N4.65.

Evaluation of the pH-responsive volume change of the mixed hydrogel: The gelator **1** and the additive **2** were mixed in test tubes in molar ratios from 0:10–10:0 and a buffer solution (25 mM Na/K phosphate buffer, pH 7.0, 0.5 mL) was added. To obtain homogenous solutions, the reaction mixtures were gently heated and then incubated at room temperature for one day. The gelation capabilities were determined by observing displacement of the gels upon inversion of the tubes. The tubes of hydrogel solutions were weighed and then incubated for 20 min in a box that contained

a tube of conc. HCl, whose vapor provided an acidic atmosphere. The tubes were then re-weighed to determine the mass and, therefore, volume of water expelled for each mixed hydrogel. After exposure to HCl vapor, the expelled water had a pH value of 1–2. The shrinkage ratio was estimated by dividing the final weight of the hydrogel by the initial weight. Macroscopic morphology changes were observed and recorded by using a digital camera.

X-ray powder diffraction: The xerogel was placed in a glass capillary tube (Φ = 0.7 mm) and the X-ray diffractogram (MAC Science M18XHF) was recorded on an imaging plate by using Cu radiation (λ = 1.54178 Å) at a distance of 15 cm.

CLSM observation: The hydrogel sample was placed on a glass substrate and covered with a cover glass. A confocal laser scanning microscope (Carl Zeiss: LSM510META) with an argon laser (excitation wavelength 488 nm) was used. Fluorescence spectra of the gel fibers were also obtained by using this microscope.

Controlled release of the entrapped substances: Vitamin B₁₂ was added to the suspension of **1** and **2b** in phosphate buffer solution (25 mM Na/K phosphate buffer, pH 7.0, 0.5 mL) and the mixture was heated to obtain a clear, homogeneous solution (vitamin B₁₂ = 0.5 mM, **1** = 3.95 mM, **2b** = 3.95 mM). After incubation at room temperature for 1 day, the hydrogel containing vitamin B₁₂ formed. This hydrogel was exposed to HCl vapor for 15 min and the expelled solution was collected, as described above. After neutralization and appropriate dilution, the concentration of the released vitamin B₁₂ was determined by using a UV/Vis spectrophotometer (Shimadzu UV2550). This method was employed for the other substances investigated.

Acknowledgement

This research was partly supported by the SHISEIDO Foundation for Science and Technology, the Tokuyama Science Foundation, the Kurata Science Foundation, and the 21st COE project on “Functional Innovation of Molecular Informatics” from the Ministry of Education, Science, Sports, and Culture, Japan.

- [1] a) Y. Furusho, T. Kimura, Y. Mizuno, T. Aida, *J. Am. Chem. Soc.* **1997**, *119*, 5267–5268; b) E. Yashima, K. Maeda, Y. Okamoto, *Nature* **1999**, *399*, 449–451; c) A. Sugasaki, M. Ikeda, M. Takeuchi, A. Robertson, S. Shinkai, *J. Chem. Soc. Perkin Trans. 1* **1999**, 3259–3264.
- [2] For reviews, see: a) A. R. Pease, J. O. Jeppesen, J. F. Stoddart, Y. Luo, C. P. Collier, J. R. Heath, *Acc. Chem. Res.* **2001**, *34*, 433–444; b) J.-P. Collin, C. Dietrich-Buchecker, P. Gaviña, M. C. Jimenez-Molero, J.-P. Sauvage, *Acc. Chem. Res.* **2001**, *34*, 477–487.
- [3] For reviews, see: a) R. Ballardini, V. Balzani, A. Credi, M. T. Gandolfi, M. Venturi, *Acc. Chem. Res.* **2001**, *34*, 445–455; b) C. A. Schalley, K. Beizai, F. Vögtle, *Acc. Chem. Res.* **2001**, *34*, 465–476; c) B. L. Feringa, *Acc. Chem. Res.* **2001**, *34*, 504–513.
- [4] C. P. Collier, G. Mattersteig, E. W. Wong, Y. Luo, K. Beverly, J. Sampaio, F. M. Raymo, J. F. Stoddart, J. P. Heath, *Science* **2000**, *289*, 1172–1175.
- [5] For reviews, see: a) Y. Osada, J.-P. Gong, *Adv. Mater.* **1998**, *10*, 827–837; b) B. Jeong, A. Gutowska, *Trends Biotechnol.* **2002**, *20*, 305–305; c) A. Lendlein, S. Kelch, *Angew. Chem.* **2002**, *114*, 2138–2162; *Angew. Chem. Int. Ed.* **2002**, *41*, 2034–2057.
- [6] a) C. Fouquey, J.-M. Lehn, A.-M. Levelut, *Adv. Mater.* **1990**, *2*, 254–257; b) R. P. Sijbesma, F. H. Beijer, L. Brunsveld, B. J. B. Folmer, J. H. K. Ky Hirschberg, R. F. M. Lange, J. K. L. Lowe, E. W. Meijer, *Science* **1997**, *278*, 1601–1604; c) R. K. Castellano, D. M. Rudkevich, J. Rebek, Jr., *Proc. Natl. Acad. Sci. USA* **1997**, *94*, 7132–7137.
- [7] a) S. Kiyonaka, K. Sugiyasu, S. Shinkai, I. Hamachi, *J. Am. Chem. Soc.* **2002**, *124*, 10954–10955; after publication of our report, another example was published: b) Y. Zhang, H. Gu, Z. Yang, B. Xu, *J. Am. Chem. Soc.* **2003**, *125*, 13680–13681.

- [8] a) T. Tanaka, *Phys. Rev. Lett.* **1978**, *40*, 820–823; b) T. Tanaka, *Sci. Am.* **1981**, *244*, 124–136; c) A. Suzuki, T. Tanaka, *Nature* **1990**, *346*, 345–347; d) M. Annaka, T. Tanaka, *Nature* **1992**, *355*, 430–432; e) T. Oya, T. Enoki, A. Y. Grosberg, S. Masamune, T. Sakiyama, Y. Takeoka, K. Tanaka, G. Wang, Y. Yilmaz, M. S. Feld, R. Dasari, T. Tanaka, *Science* **1999**, *286*, 1543–1545; f) T. Enoki, K. Tanaka, T. Watanabe, T. Oya, T. Sakiyama, Y. Takeoka, K. Ito, G. Wang, M. Annaka, K. Hara, R. Du, J. Chuang, K. Wasserman, A. Y. Grosberg, S. Masamune, T. Tanaka, *Phys. Rev. Lett.* **2000**, *85*, 5000–5003.
- [9] a) A. Aggeli, M. Bell, N. Boden, J. N. Keen, P. F. Knowles, T. C. B. McLeish, M. Pitkeathly, S. E. Radford, *Nature* **1997**, *386*, 259–262; b) W. A. Petka, J. L. Harden, K. P. McGrath, D. Wirtz, D. A. Tirrell, *Science* **1998**, *281*, 389–392; c) L. A. Estroff, A. D. Hamilton, *Angew. Chem.* **2000**, *112*, 3589–3592; *Angew. Chem. Int. Ed.* **2000**, *39*, 3447–3450; d) J. H. Collier, B.-H. Hu, J. W. Ruberti, J. Zhang, P. Shum, D. H. Thompson, P. B. Messersmith, *J. Am. Chem. Soc.* **2001**, *123*, 9463–9464; e) U. Maitra, S. Mukhopadhyay, A. Sarkar, P. Rao, S. S. Indi, *Angew. Chem.* **2001**, *113*, 2341–2343; *Angew. Chem. Int. Ed.* **2001**, *40*, 2281–2283; f) A. P. Nowak, V. Breedveld, L. Pakstis, B. Ozbas, D. J. Pine, D. Pochan, T. J. Deming, *Nature* **2002**, *417*, 424–428; g) J. P. Schneider, D. J. Pochan, B. Ozbas, K. Rajagopal, L. Pakstis, J. Kretsinger, *J. Am. Chem. Soc.* **2002**, *124*, 15030–15037; h) R. Iwaura, K. Yoshida, M. Masuda, K. Yase, T. Shimizu, *Chem. Mater.* **2002**, *14*, 3047–3053; i) S. R. Haines, R. G. Harrison, *Chem. Commun.* **2002**, 2846–2847; j) H. Kobayashi, A. Friggeri, K. Koumoto, M. Amaike, S. Shinkai, D. N. Reinhoudt, *Org. Lett.* **2002**, *4*, 1423–1426; k) D. J. Pochan, J. P. Schneider, J. Kretsinger, B. Ozbas, K. Rajagopal, L. Haines, *J. Am. Chem. Soc.* **2003**, *125*, 11802–11803; l) M. Suzuki, M. Yumoto, M. Kimura, H. Shirai, K. Hanabusa, *Chem. Eur. J.* **2003**, *9*, 348–354; m) S. M. Park, Y. S. Lee, B. H. Kim, *Chem. Commun.* **2003**, 2912–2913; n) S. Kiyonaka, S.-L. Zhou, I. Hamachi, *Supramol. Chem.* **2003**, *15*, 521–528; o) K. J. C. van Bommel, C. van der Pol, I. Muizebelt, A. Friggeri, A. Heeres, A. Meetsma, B. L. Feringa, J. van Esch, *Angew. Chem.* **2004**, *116*, 1695–1699; *Angew. Chem. Int. Ed.* **2004**, *43*, 1663–1667; p) for an excellent review on a low-molecular-weight hydrogelator, see: L. A. Estroff, A. D. Hamilton, *Chem. Rev.* **2004**, *104*, 1201–1217.
- [10] For supramolecular organogels, see: a) K. Hanabusa, T. Miki, Y. Taguchi, T. Koyama, H. Shirai, *J. Chem. Soc. Chem. Commun.* **1993**, 1382–1384; b) K. Murata, M. Aoki, T. Suzuki, T. Harada, H. Kawabata, T. Komori, F. Ohseto, K. Ueda, S. Shinkai, *J. Am. Chem. Soc.* **1994**, *116*, 6664–6676; c) P. Terech, R. G. Weiss, *Chem. Rev.* **1997**, *97*, 3133–3159; d) J. H. van Esch, B. L. Feringa, *Angew. Chem.* **2000**, *112*, 2351–2354; *Angew. Chem. Int. Ed.* **2000**, *39*, 2263–2266.
- [11] S. Kiyonaka, K. Sada, I. Yoshimura, S. Shinkai, N. Kato, I. Hamachi, *Nat. Mater.* **2004**, *3*, 58–64.
- [12] For two-component supramolecular gels, see: a) K. Hanabusa, T. Miki, Y. Taguchi, T. Koyama, H. Shirai, *J. Chem. Soc. Chem. Commun.* **1993**, 1382–1384; b) Z. Yang, H. Gu, Y. Zhang, L. Wang, B. Xu, *Chem. Commun.* **2004**, 208–209.
- [13] a) I. Hamachi, S. Kiyonaka, S. Shinkai, *Chem. Commun.* **2000**, 1281–1282; b) I. Hamachi, S. Kiyonaka, S. Shinkai, *Tetrahedron Lett.* **2001**, *42*, 6141–6145; c) S. Kiyonaka, S. Shinkai, I. Hamachi, *Chem. Eur. J.* **2003**, *9*, 976–983.
- [14] Molecular modeling was performed on the basis of the X-ray crystallographic data of **1** with the assumption that all methylene chains form trans conformations.
- [15] We confirmed that compound **1** was not chemically decomposed under these conditions, by using TLC, MALDI-TOF mass spectroscopy, and ¹H NMR spectroscopy of the sample after the acidic treatment (See Supporting Information, Figure S1). This is also supported by the repeated shrinkage/swelling cycles of the mixed hydrogel.
- [16] See Supporting Information, Figure S2. In Figure 2 there is an additional peak in the XRD spectrum of the swollen gel, which may be due to the inclusion of phosphate salt within the gel.
- [17] This may suggest good miscibility of these two components in the mixed hydrogel (**1/2** = 10:10), supported by the ¹H NMR spectra, which show that the molecular ratio (**1/2**) in the mixed hydrogel before and after shrinkage was practically unchanged.
- [18] O. Gershevit, C. N. Sukenik, *J. Am. Chem. Soc.* **2004**, *126*, 482–483.
- [19] J. C. Tiller, *Angew. Chem.* **2003**, *115*, 3180–3183; *Angew. Chem. Int. Ed.* **2003**, *42*, 3072–3075.
- [20] a) S. Zhang, *Nat. Biotechnol.* **2003**, *21*, 1171–1178; b) S. Zhang, *Nat. Mater.* **2004**, *3*, 7–8.

Received: July 3, 2004

Published online: December 27, 2004